Journal for Multiscale Computational Engineering, 12 (5): 411–421 (2014)

DISLOCATION CORE RECONSTRUCTION BASED ON FINITE DEFORMATION APPROACH AND ITS APPLICATION TO 4H-SiC CRYSTAL

Jan Cholewiński, Marcin Maździarz, Grzegorz Jurczak, & Paweł Dłużewski***

Department of Computational Science, Institute of Fundamental Technological Research, Polish Academy of Sciences, Pawińskiego 5b, 02-106 Warsaw, Poland

*Address all correspondence to Jan Cholewiński, E-mail: jcholew@ippt.gov.pl

A proper reconstruction of discrete crystal structure with defects is an important problem in dislocation theory. Currently, procedures for dislocation core reconstruction presented in the literature usually neglect configuration changes. The present paper discusses a new approach, which uses an iterative algorithm to determine an atomistic configuration of the dislocation core. The mathematical background is based on finite deformation theory, in which an iterative algorithm searches for the new atomic configuration corresponding to the actual atomic configuration of the deformed crystal. Its application to the reconstruction of 4H-SiC crystal affected by the system of four threading dislocations is presented as an example. Molecular statics calculations suggest a lower potential energy, as well as dislocation core energy, per-atom energy, and per-atom stresses for the structure reconstructed by use of the iterative algorithm against the classical solution based on the Love's equations.

KEY WORDS: *dislocation, dislocation core energy, finite deformation, molecular statics*

1. INTRODUCTION

Dislocations and their long-range elastic deformation field play an important role in the prediction of various physical properties of crystal structures. For example, the mechanism of plastic deformation is closely related to the behaviour of crystallographic defects (Hirth and Lothe, 1982). This concerns as well semiconductor crystals (e.g., silicon carbide and III-V nitrides – very promising semiconducting materials for electronic industry) where threading dislocations (TDs) compose nonradiative recombination centers (Wright and Grossner, 1998). Also, an emission spectrum which is a very important parameter for the optoelectronic device depends on the formation energy related to the atomic configuration of the dislocation core (Belabbas et al., 2011; Béré et al., 2002; Blumenau et al., 2003). Despite the very promising electronic properties of these semiconductors, the nonradiative recombination as well as residual stresses around defect formations which arise during the growth process, compose a technological barrier for the application of such materials in electronic and optoelectronic devices. Experimental measurement in that domain, mainly by transmission electron microscopy (TEM) (Dasilva et al., 2010; Liu et al., 2002; Persson et al., 2002) are very tricky, therefore atomistic simulations have become a common method for investigating dislocation phenomena in dislocation theory. Despite real crystals demonstrate an anisotropic behavior, currently the most popular analytical approach based on the Love's equations (Love, 1927) and its various modifications (de Wit, 1973; Hirth and Lothe, 1982; Read Jr., 1953) covers the isotropic continuum. The main reason for that situation is a relatively small difference between isotropic and fully the anisotropic solution, which by itself does not justify investigating the more complex problem (Steeds, 1973). Nevertheless, an inaccurate atomistic configuration in the modeling of the dislocation core makes interpretation of results more difficult. Here, a relatively simple iterative procedure within the framework of finite deformation theory is proposed. This approach, which has a classical solution to Love's equations as a starting configuration, improves on the accuracy of the reconstruction of the dislocation core.

1543–1649/14/$35.00

This article is organized as follows. Sections 2–4 describe the theoretical background and mathematical foundations of the iterative algorithm for the atomistic reconstruction of dislocation structure. The next sections describe an application of the methodology on the basis of TDs in 4H-SiC crystal. In particular, Section 5 deals with molecular simulations of crystal sample, and Section 6 presents an analysis of numerical results. In Section 7 a short discussion of the results is given.

2. INTRODUCTION TO THE CONTINUUM THEORY OF DISLOCATIONS

To take into account the initial incompatibilities, after Kröner (1981); Teodosiu (1970), an additional intermediate (local lattice reference) configuration has been introduced. For crystal heterostructure, the total deformation gradient $\mathbf{F}_{\mathrm{tot}}$ can be therefore decomposed multiplicatively into the lattice and plastic deformation tensors as follows:

$$\mathbf{F}_{\mathrm{tot}} = \mathbf{F}\,\mathbf{F}_{\mathrm{pl}}\,. \tag{2.1}$$

The lattice deformation $\mathbf{F}$ corresponds to an elastic relaxation of chemically nonhomogeneous heterostructure, while $\mathbf{F}_{\mathrm{pl}}$ denotes the permanent rearrangement of the crystal structure caused by lattice incompatibilities, e.g., dislocations (Dłużewski et al., 2004, 2010). In this paper, chemically homogeneous crystals are dealt with, and therefore chemical deformation can be neglected. Hence, elastic and plastic deformations appear only. Generally, after applying initial incompatibilities prescribed by the plastic deformation tensor, the initial configuration is somewhat difficult to use. Therefore, the intermediate configuration will be used as a local reference configuration for the elastic deformation tensor. In that convention, the so-called true Burgers vector $\widehat{\mathbf{b}}$, which represents the magnitude and direction of the lattice distortion, in local reference configuration can be written as

$$-\widehat{\mathbf{b}} = \oint_{\mathrm{C}} d\mathbf{X} = \oint_{\mathrm{o}} \mathbf{F}^{-1} d\mathbf{x} = \oint_{\mathrm{o}} (\mathbf{1} - \boldsymbol{\beta})\, d\mathbf{x}\,. \tag{2.2}$$

The integration of lattice distortions can be performed over closed (C) or open circuit (o) in the local reference (relaxed – $\mathrm{d}\mathbf{X}$) or actual (deformed – $\mathrm{d}\mathbf{x}$) configuration. The lattice distortion tensor $\boldsymbol{\beta}$ is related to the lattice spacings in the actual configuration ($\partial\mathbf{u}/\partial\mathbf{x}$) and can be transformed to the local reference configuration according to the following transformation rule:

$$\widehat{\boldsymbol{\beta}} = (\mathbf{1} - \boldsymbol{\beta})^{-1} - \mathbf{1}. \tag{2.3}$$

The lattice deformation and distortion tensors satisfy the following mutually reversible relations:

$$\mathbf{F} = \frac{\partial(\mathbf{X} + \mathbf{u})}{\partial \mathbf{X}} = \mathbf{1} + \widehat{\boldsymbol{\beta}} \quad \text{and} \quad \mathbf{F}^{-1} = \frac{\partial(\mathbf{x} - \mathbf{u})}{\partial \mathbf{x}} = \big(\mathbf{1} - \boldsymbol{\beta}\big)^{-1}. \tag{2.4}$$

3. ANALYTICAL EQUATIONS OF A STRAIGHT-LINE DISLOCATION

The elastic displacement field around dislocation, in the case of straight-line dislocation with mixed type of the Burgers vector [after Love (1927)] and its further modifications (de Wit, 1973; Hirth and Lothe, 1982; Read Jr., 1953) for isotropic material, can be written in the following form

$$\begin{aligned} u_1 &= \frac{b_1}{2\pi}\left[\operatorname{atan2}\frac{x_2}{x_1} + \frac{x_1 x_2}{2(1-\nu)(x_1^2+x_2^2)}\right], \\ u_2 &= -\frac{b_1}{2\pi}\left[\frac{1-2\nu}{4(1-\nu)}\ln\frac{x_1^2+x_2^2}{r_\circ^2} + \frac{x_1^2-x_2^2}{4(1-\nu)(x_1^2+x_2^2)}\right], \\ u_3 &= \frac{b_3}{2\pi}\operatorname{atan2}\frac{x_2}{x_1}, \end{aligned} \tag{3.1}$$

where b_1, b_3, and ν denote, respectively, edge, screw components of the Burgers vector, and the Poisson ratio. Components of the Burgers vector are coaxial with axes x_1 and x_3 of the coordinate system ($b_2 = 0$). The radius $r_\circ$ is

used here to normalize the vertical shift in the dislocation core. The formulas presented above allow us to introduce perfect or partial dislocation in a slip, climb, or mixed way. The $atan2$ function is defined according to the following convention:

$$\text{atan2}\,\frac{x_2}{x_1} = \begin{cases} \arctan\dfrac{x_2}{x_1} & \text{for } x_1 > 0, \\ \arctan\dfrac{x_2}{x_1} + \pi & \text{for } x_2 \geq 0,\ x_1 < 0, \\ \arctan\dfrac{x_2}{x_1} - \pi & \text{for } x_2 < 0,\ x_1 < 0, \\ 0 & \text{for } x_1 = 0. \end{cases}$$

Differentiation of Eqs. (3.1) give the following formulas for lattice distortions ($\boldsymbol{\beta} = \partial\mathbf{u}/\partial\mathbf{x}$):

$$\begin{aligned} \beta_{11} &= \frac{-b_1}{2\pi}\,\frac{(3-2\nu)\,x_1^2x_2 + (1-2\nu)\,x_2^3}{2(1-\nu)(x_1^2+x_2^2)^2}\,, & \beta_{12} &= \frac{b_1}{2\pi}\,\frac{(3-2\nu)\,x_1^3 + (1-2\nu)\,x_1x_2^2}{2(1-\nu)(x_1^2+x_2^2)^2}\,, \\ \beta_{21} &= \frac{-b_1}{2\pi}\,\frac{(1-2\nu)\,x_1^3 + (3-2\nu)\,x_1x_2^2}{2(1-\nu)(x_1^2+x_2^2)^2}\,, & \beta_{22} &= \frac{b_1}{2\pi}\,\frac{(1+2\nu)\,x_1^2x_2 - (1-2\nu)\,x_2^3}{2(1-\nu)(x_1^2+x_2^2)^2}\,, \\ \beta_{31} &= \frac{-b_3}{2\pi}\,\frac{x_2}{x_1^2+x_2^2}\,, & \beta_{32} &= \frac{b_3}{2\pi}\,\frac{x_1}{x_1^2+x_2^2}\,. \end{aligned} \tag{3.2}$$

This approach uses small deformation theory and neglects the differences between the initial, actual, and lattice reference configurations. Regardless of such limitations, many useful results and analytical formulas have been obtained on that basis.

4. ATOMISTIC RECONSTRUCTION OF DISLOCATION CORES

To hold the symmetry of atomic positions in dislocation core, the lattice distortion has to be related to the actual configuration. However, it is not possible to start the process of dislocation reconstruction from the actual (wanted) configuration; it always starts from the initial one. In other words, because the actual configuration is unknown, instead of the "pull back" displacement field $\mathbf{u} = \mathbf{f}(\mathbf{x})$, the "push forward" analytical formula is applied, which corresponds to

$$\mathbf{u} = \mathbf{f}(\mathbf{X})\,. \tag{4.1}$$

In effect, a broken symmetry for the actual configuration of the lattice distortion field appears. Of course, the deviation from the correct (symmetric) distortion field for a single dislocation is hardly visible. In the case of dislocation networks, deviation accumulates step-by-step during sequential dislocation introduction and meaningful error arises, e.g., for lattice mismatch dislocations. To avoid this error, another displacement function, consistent with Eqs. (3.1) must be used. From a mathematical perspective, the wanted analytical function $\overline{\mathbf{f}}$, which introduces a proper distortion field directly from the perfect lattice, should satisfy the following condition:

$$\mathbf{u} = \overline{\mathbf{f}}(\mathbf{X}) = \mathbf{f}\big(\mathbf{X} + \mathbf{u}\big)\,, \tag{4.2}$$

where $\mathbf{f}(\cdot)$ is the same as in Eq. (4.1). An analytical solution for the above implicit equation set, with respect to $\overline{\mathbf{f}}(\cdot)$, for a given $\mathbf{f}(\cdot)$ is not a trivial mathematical problem. For now, to the authors' best knowledge, no analytical formulas for the function $\overline{\mathbf{f}}(\cdot)$ exist. Despite arising difficulties, Eq. (4.2) can be estimated numerically by means of iterative methods. To do this, let us consider the displacement vector of an atom at initial position $\mathbf{X}$. The displacement vector corresponding to its position can be determined by use of the following iterative formula:

$$\mathbf{u}^{i+1} = \mathbf{u}^i + \Delta\mathbf{u}^{i+1}\,, \tag{4.3}$$

where i means iteration step. The Newton–Raphson algorithm, assumes the correction $\Delta\mathbf{u}$ equal to

$$\Delta\,\mathbf{u}^{i+1} = -\left[\frac{\partial\Psi(\mathbf{X},\mathbf{u})}{\partial\mathbf{u}}\right]^{-1}_{\mathbf{u}=\mathbf{u}^i}\Psi(\mathbf{u}^i)\,, \tag{4.4}$$

where the correction factor Ψ is

$$\Psi(\mathbf{X},\mathbf{u}) = \mathbf{u} - \mathbf{f}(\mathbf{X}+\mathbf{u})\,. \tag{4.5}$$

Differentiation of the correction factor over the displacement field [we may write $\mathrm{d}\mathbf{u} = \mathrm{d}(\mathbf{X}+\mathbf{u})$] leads to a formula for the tangent matrix

$$\frac{\partial\Psi(\mathbf{X},\mathbf{u})}{\partial\mathbf{u}} = \mathbf{1} - \boldsymbol{\beta}(\mathbf{x}). \tag{4.6}$$

Finally, correction for the displacement vector at the $(\mathrm{i}+1)$-th step of the iterative scheme is as follows:

$$\Delta\,\mathbf{u}^{i+1} = -\big[\mathbf{1} - \boldsymbol{\beta}(\mathbf{X}+\mathbf{u}^{i})\big]^{-1}\big[\mathbf{u}^{i} - \mathbf{f}(\mathbf{X}+\mathbf{u}^{i})\big], \tag{4.7}$$

where displacements $\mathbf{f}(\cdot)$ and distortions $\boldsymbol{\beta}(\cdot)$ are calculated on the basis of classical equations [Eqs. (3.1) and (3.2)] in the updated configuration $(\mathbf{X}+\mathbf{u})$. Nonlinear equation set (4.2) was solved by use of modified Powell's hybrid method (Galassi et al., 2002). At each iteration step, the standard Newton iteration is performed first. If the solution leaves a so-called "trusted region" of the values, then linear combinations of the Newton iteration and conjugate gradient method are employed. Due to the specifics of the proposed methodology, and mainly due to the given form of the Love's equations (3.1), the iterative procedure measurably improves the accuracy of the dislocation configuration in the case of edge or mixed dislocation. Screw dislocation configuration is not affected by iterative procedure at all. The reason for this is that the u_3 component of the displacement field does not depend on x_3 position, nor does the b_3 component of the Burgers vector affects u_1, u_2 displacements.

5. MOLECULAR SIMULATIONS

To verify the methodology proposed in Section 4, molecular calculations were performed for a 4H-SiC crystal affected by four threading dislocations, see Fig. 1. The sample is assumed to be rhombic in shape, one lattice parameter thick, and consist of 79,524 elementary cells (282 $\times$ 282). The quite large size of the sample reduces the mutual influence of neighboring dislocations. Dislocation lines impinge the sample's plane and coincide with the orientation of the crystal c axis. The dislocation core is assumed arbitrary in the center of 4H-SiC elementary cell, see Fig. 1(b). A set of four dislocations, consecutively edge, mixed, and screw type, were inserted into the sample by use of the classical (linear) method and the iterative one. In the case of 4H-SiC crystal the Burgers vector of a perfect dislocation is equal to 3.073 Å or 10.053 Å, respectively, for the edge and screw type. The mixed dislocation used here is geometrical superposition of the perfect edge and screw dislocations. The inserted dislocations are of the same type but their Burgers vectors are, by pairs, mutually opposite. Finally, periodic boundary conditions for the surfaces have been

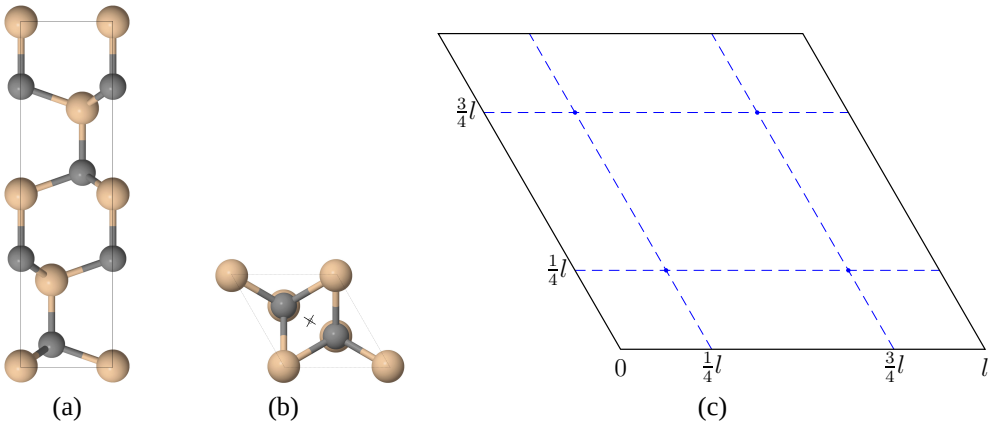

FIG. 1: Ball and stick model of a 4H-SiC elementary cell (beige – Si, gray – C) in **(a)** $[\bar{1}2\bar{1}0]$, **(b)** [0001] projection, and **(c)** plain view of the sample with dislocation positions (where the dashed lines intersect)

applied and an analogical, molecular calculation was performed for each dislocation type. Energy of the sample has been determined and hence the energy of the dislocation core by use of a perfect crystal sample as a reference system. The following cases were studied:

i. system of four edge dislocations (Fig. 2)

ii. system of four mixed dislocations

iii. system of four screw dislocations (Fig. 3)

Though iterative methodology does not affect the pure screw dislocations, it is presented here (shared configuration with linear approach) just to gather all types of dislocations. Since we are interested in the quasi-static behavior of the crystal, a molecular statics (MS) approach (Maździarz et al., 2010, 2011; Tadmor and Miller, 2011) rather than molecular dynamics (MD) was used. MS is more adequate here to deal with dislocation core configurations. All molecular calculations were performed by making use of the large-scale atomic/molecular massively parallel simulator (LAMMPS) (Plimpton, 1995) and visualized in the Open Visualization Tool (OVITO) (Stukowski, 2010). Energy minimization with periodic boundary condition applied to all facets of the sample was performed with the Polak–Ribiere version of the conjugate gradient algorithm. Convergence is achieved when the relative change in the energy and forces between two consecutive iterations is less than 10^{-13}. After the energy minimization process an external pressure was applied to the simulation box to examine the effect of the volume change. This allows the simulation box volume and shape to vary during the iterations of the minimizer (Plimpton, 1995). The effect of the volume change seems to be constant for all calculated samples (perfect as well as defected) and it is ~ 300 eV (against 4,032,645 eV of the total energy for the perfect sample). Therefore, we attribute that negligible effect to the deficiency of the used potential, and follow-up we do not take into account. To model 4H-SiC crystal an empirical Tersoff potential, parametrized by Erhart (Erhart and Albe, 2005) was used, which reproduces stiffness coefficients with reasonable accuracy: C_{11} = 485 GPa, C_{12} = 123 GPa, C_{13} = 64 GPa, C_{33} = 544 GPa, and C_{44} = 160 GPa. The total potential energy for the whole sample is not a very informative parameter, especially in terms of dislocation core energy. Therefore, to acquire more information about the dislocation energy local atom values were used, i.e., the so-called per-atom potential energy and per-atom stress tensor concepts adopted from LAMMPS.

On the basis of the continuum theory of dislocations (Hirth and Lothe, 1982), the total energy of the crystal with a TD (energy density per dislocation length) can be additively decomposed into an elastic part and inelastic energy stored in the core E^c

$$E = \begin{cases} E^c, & R < R_c\,, \\ E^c + A \cdot \ln\left(\dfrac{R}{R_c}\right), & R \geq R_c\,, \end{cases} \tag{5.1}$$

where the prelogarithmic coefficient A depends on the length of the Burgers vector and the crystal stiffness (Hirth and Lothe, 1982; Schoeck, 1995). The elastic part of the energy comes from the deformation of bonds outside the dislocation core defined by a cylinder of radius R_c. The core energy is the effect of permanent rearrangement of the atomic bonds. The energy of the dislocation can be calculated as a difference between the energy of the structure with defects E^D and the reference crystal E^P. Hence, the total energy per unit length l, stored in the cylinder V_R can be expressed as

$$E = \frac{1}{l} \sum_{i \in V_R} (E_i^D - E_i^P)\,, \tag{5.2}$$

where i means summation over atoms. Some authors (Belabbas et al., 2011) use an approximated, graphical analysis of the total energy graphs to determine the core radius R_c. Due to the high level of discretion during that analysis, here the core radius R_c is assumed to be equal to the Burgers vector.

6. RESULTS AND DISCUSSION

For a given potential (Erhart and Albe, 2005) the total energy of the perfect crystal E^P is equal to $-$4,032,645 eV. Our sample consists of 636,192 atoms, which leads to the reference per-atom energy ${E_i}^P = -6.34$ eV, see Figs. 2–3. Increase of the energy caused by dislocations varies greatly on the dislocation type. Calculated energies of the

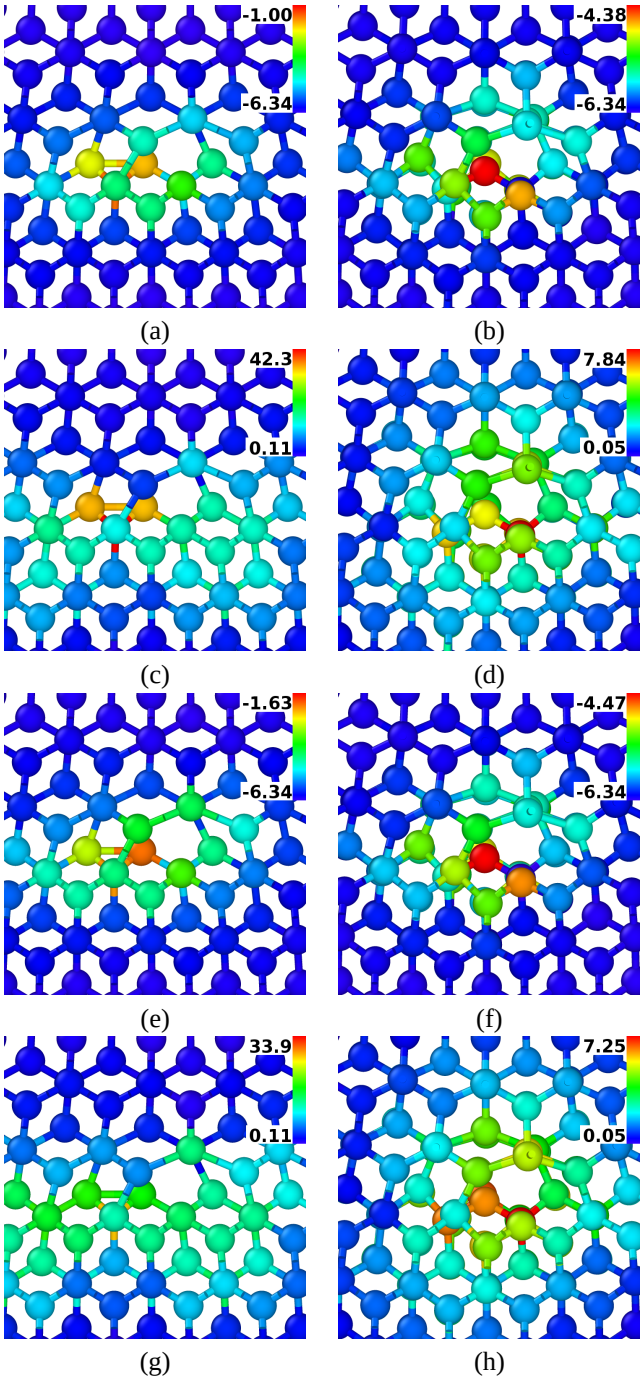

FIG. 2: Ball and stick model of the local vicinity (12Å $\times$ 12 Å) of the edge TD inserted into the 4H-SiC crystal by use of the linear method **(a)**–**(d)** and iterative one **(e)**–**(h)**. Per-atom energy (eV) is visualized in the initial configuration (a),(e) and relaxed one (b),(f). Per-atom stresses [10^6 MPa Å^3, see Plimpton (1995) for units description] are given in the initial configuration (c),(g) and relaxed one (d),(h).

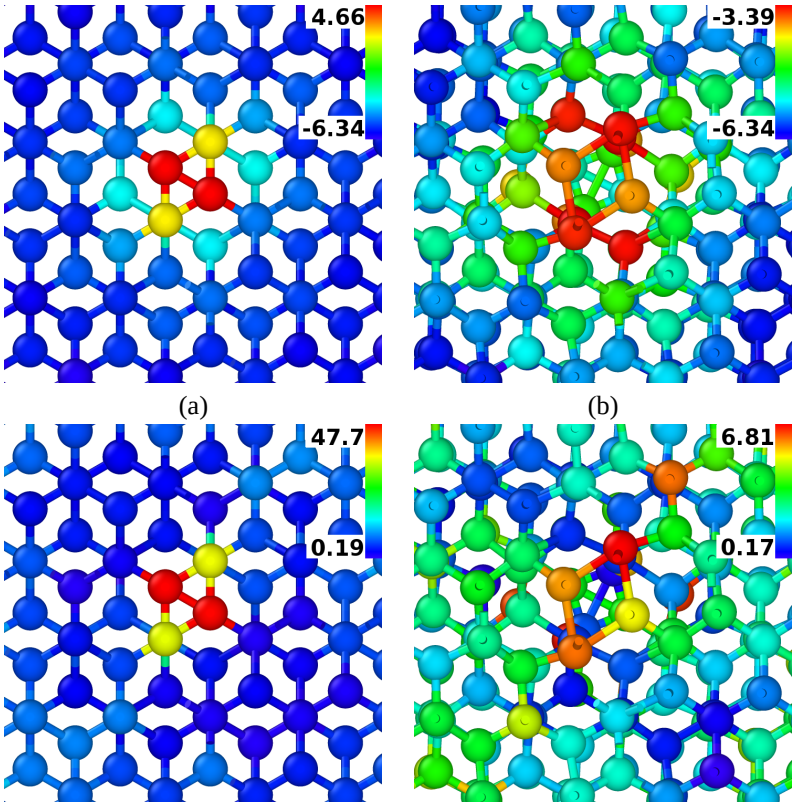

FIG. 3: Ball and stick model of the local vicinity of the screw TD. Per-atom energy (eV) is visualized in the initial configuration **(a)** and relaxed one **(b)**. Per-atom stresses (10^6 MPa Å^3) are given in the initial configuration **(c)** and relaxed one **(d)**.

sample with dislocations, energy differences and number of iterations to reach convergence are presented in Table 1. By plotting energy density charts (Fig. 4) and fitting energy formula (5.1), we have determined core energies E^c and prelogarithmic factors A, see Table 2. Theoretical predictions for factor A_{th} are also given here. General comparison of the total energy, per-atom energy, and per-atom stresses is difficult; therefore, we focus on the effect of the insertion procedure. Let us here encapsulate results, in order for edge, mixed, and screw dislocations.

TABLE 1: Total potential energy calculated for the sample with different type of dislocations and different way of reconstruction. E_0 means value at initial configuration (just after reconstruction), E_f – after relaxation. Differences in energy against the perfect structure (E^P) and number of iteration to reach the tolerance are also given

Dislocation type	**Insertion**	E_0 **(eV)**	E_f **(eV)**	$E_0 - E^P$ **(eV)**	$E_f - E^P$ **(eV)**	**Iterations**
Edge	Linear	−4,031,618	−4,032,328	1027.4	317.5	2970
	Iterative	−4,031,640	−4,032,332	1005.4	313.1	2934
Mixed	Linear	−4,024,478	−4,030,574	8167	2070.6	3114
	Iterative	−4,024,565	−4,030,598	8079.6	2047.2	3055
Screw		−4,025,689	−4,030,746	6956	1899	2866

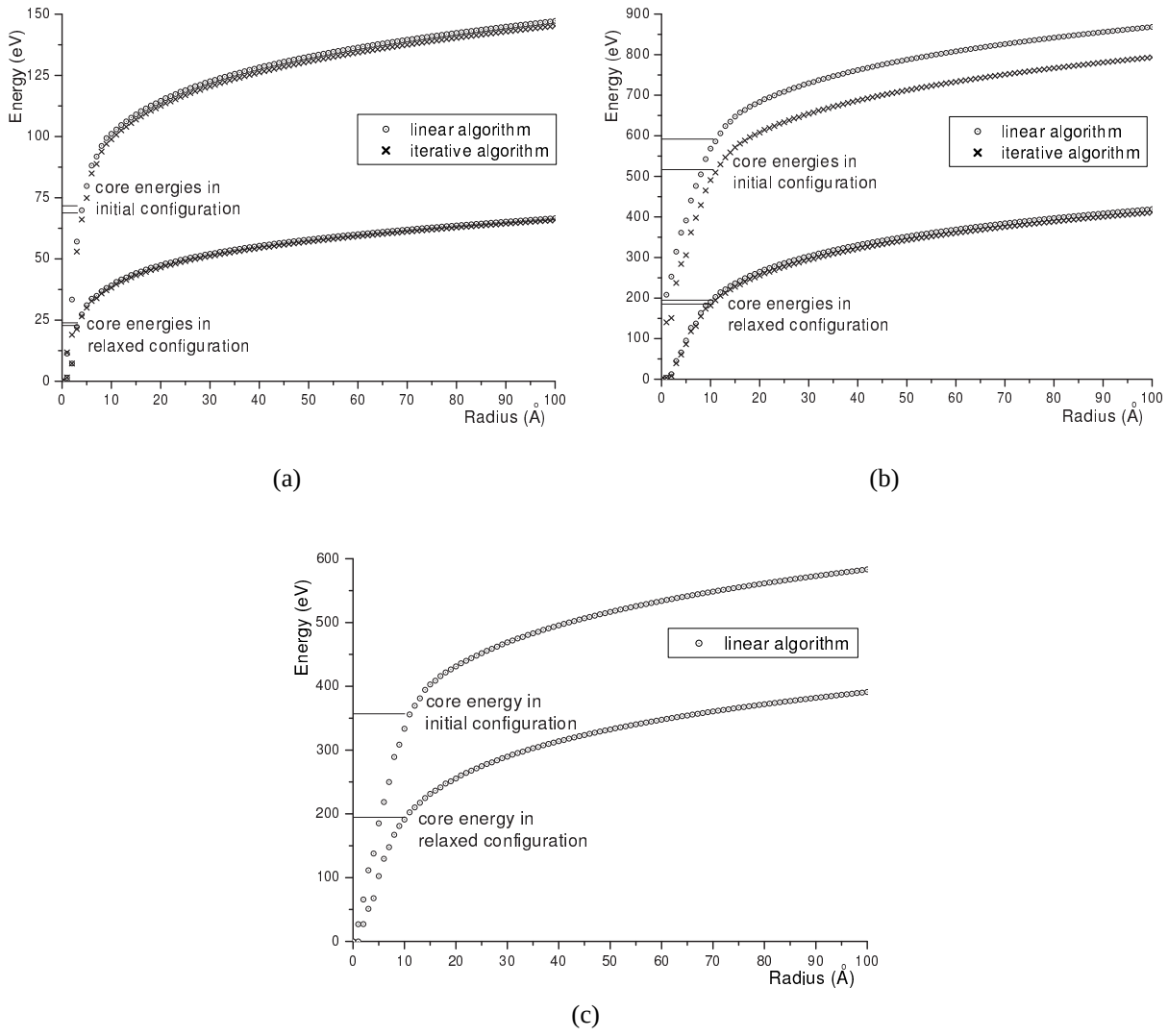

FIG. 4: Total energy stored in a cylinder of radius R [and 10 Åheight, see Eq. (5.2)] for **(a)** edge TD, **(b)** mixed TD, and **(c)** screw TD. Core energy and core radius for each configuration is indicated by a horizontal line.

TABLE 2: Dislocation core energies E^c and prelogarithmic coefficients A for different types of dislocations and different way of reconstruction. ${E^c}_0$ and A_0 mean values at initial configuration, while ${E^c}_f$, A_f – after relaxation. A_{th} denotes theoretical prediction (Hirth and Lothe, 1982)

Dislocation type	**Insertion**	${E^c}_0$ **(eV/Å)**	${E^c}_f$ **(eV/Å)**	A_0 **(eV/Å)**	A_f **(eV/Å)**	A_{th} **(eV/Å)**
Edge	Linear	7.17	2.39	2.15	1.21	1.06
	Iterative	6.88	2.28	2.17	1.22	
Mixed	Linear	59.20	19.48	11.86	9.69	9.09
	Iterative	51.65	18.53	11.90	9.74	
Screw		35.69	19.46	9.74	8.46	8.04

i. Sample with edge $1/3\,\langle 11\bar{2}0\rangle$ TDs, see Fig. 2. The iterative procedure reconstructs the atomic structure with energy lower by 22 eV against the linear approach. After relaxation that difference is reduced to 3.6 eV. Dislocation core energy in the initial E_0^c and relaxed configuration E_f^c is lower in the case of the iterative approach. Conversely, the prelogarithmic factors A_0 and A_f are slightly lower for the linear method. Generally, the crystal structures after relaxation are rather similar with small advantage for the results generated by the iterative approach. Per-atom energy and per-atom stresses are lower for the iterative algorithm, both in the initial and the relaxed configuration.

ii. Sample with mixed $1/3\,\langle 11\bar{2}3\rangle$ TDs. The iterative procedure reconstructs atomic structure with energy lower by 87 eV against the linear approach. After relaxation the difference in energy is reduced to 24 eV. Dislocation core energy E^c is lower in the case of the iterative procedure, while the prelogarithmic factor A seems to be slightly lower for the linear approach. Per-atom energy for the iterative algorithm reaches 4.21 eV in the initial configuration and -3.20 eV after relaxation. The linear approach reconstructs crystal structure with energies, respectively, 5.01 and -3.13 eV. Per-atom stresses in the case of iterative algorithm are equal to 44.3×10^6 in the initial configuration and 7.4×10^6 MPa Å^3 after relaxation. Linear approach gives, respectively, 52.9×10^6 and 9.1×10^6 MPa Å^3.

iii. Sample with screw $\langle 0001\rangle$ TDs (shared configuration for both methods of dislocation insertion), see Fig. 3. Increase of the energy caused by dislocations is equal to 1899 eV. Dislocation core energy in the initial configuration is equal to 35.69 eV/Å and 19.46 eV/Å after relaxation. The prelogarithmic factor A is equal to 9.74 eV/Å in the initial configuration and 8.46 eV/Å after relaxation. Per-atom energy reaches 4.66 and -3.39 eV, respectively, for the initial configuration and relaxed one. Per-atom stresses are equal to, respectively, 47.7×10^6 and 6.8×10^6 MPa Å^3.

Core energies for dislocations in the basal plane of the 2H-SiC crystal ares reported in Blumenau et al. (2003). Energy for 90° Shockley is reported to be in the range 0.46–0.54 eV/Å or 1.03–1.13 eV/Å, depending on the terminating atom. Our results for the edge TD suggest 2.28–2.39 eV/Å. To compare these values we have to take into account the Burgers vector effect. If we assume that core energy is the quadratic function of the Burgers vector (Schoeck, 1995), our results fit in directly with updated range of the energy, namely 1.38–1.62 eV/Å and 3.06–3.39 eV/Å. In the case of mixed dislocation (30° Shockley in (Blumenau et al., 2003) while 17° TD in our case), the core energy is reported in the range 0.45–0.78 eV/Å. After conversion (Burgers vectors ratio gives the multiplier $\sim$35), dislocation core energy should be in the range 15.8–27.4 eV/Å, which corresponds with our predictions (18.53–19.48 eV/Å). Dislocation core energy for the perfect screw TD in GaN crystal is reported in Belabbas et al. (2011). DFT calculations predict core energy in the range 2.78–4.14 eV/Å. The energy calculated here is equal to 19.46 eV/Å. In the case of direct comparison of dislocations in 4H-SiC and GaN crystals, except the Burgers vector (10.053 Å against 5.185 Å), we also have to take into account different stiffness of the crystals (Schoeck, 1995) (160 GPa against 105 GPa in the case of C_{44}). Hence, core energy calculated here should fit in with a 15.9–23.7 eV/Å range of energy. Energy interpolation [Eq. (5.2)] around the dislocation core also shows good agreement with theoretical predictions. The error varies from 5% (9.74 eV/Å against 9.09) in the case of screw TD to 15% (1.22 eV/Å against 1.06) in the case of edge TD.

7. CONCLUSIONS

Described in Section 4, the iterative algorithm of dislocation reconstruction allows us to put single dislocation or dislocation network into the crystal structure. Symmetry of the lattice distortion field is preserved despite direct transformation from the initial configuration (perfect crystal) to the actual (wanted) one. Energy of the 4H-SiC sample reconstructed by means of the iterative algorithm is lower against the energy of the sample generated by the use of a linear approach. Differences in potential energy of the sample are visible even after relaxation. Also, convergence of the energy minimization algorithm is noticeably better in the iterative approach favor. Lower energy of the sample results in lower dislocation core energy, per-atom energy, as well per-atom stresses. The prelogarithmic factor is almost the same for both the iterative and linear approach.

ACKNOWLEDGMENTS

The atomistic reconstruction scheme has been implemented in the Visual Editor of Crystal Defects program (Cholewiński and Dłużewski, 2013) developed in the framework of the grant N N519 6476 40. The research was partially supported by the Polish Government (MNiSW) within the SICMAT Project financed under the European Founds for Regional Development (contract no. UDA-POIG.01.03.01-14-155/09). Additional support was provided through the Interdisciplinary Centre for Mathematical and Computational Modelling of Warsaw University (ICM UW) and the computing cluster GRAFEN at Biocentrum Ochota.

REFERENCES

Belabbas, I., Chen, J., and Nouet, G., A new atomistic model for the threading screw dislocation core in wurtzite gan, *Comput. Mater. Sci.*, vol. **51**, pp. 206–216, 2011.

Béré, A., Chen, J., Ruterana, P., Serra, A., and Nouet, G., The atomic configurations of the $\vec{a}$ threading dislocation in gan, *Comput. Mater. Sci.*, vol. **24**, pp. 144–147, 2002.

Blumenau, A. T., Fall, C. J., Jones, R., Oberg, S., Frauenheim, T., and Briddon, P. R., Structure and motion of basal dislocations in silicon carbide, *Phys. Rev. B*, vol. **68**, pp. 174108-1–174108-14, 2003.

Cholewiński, J. and Dłużewski, P., VECDs (Visual Editor of Crystal Defects) v. 0.4.2 (http://vecds.sourceforge.net), 2013.

Dasilva, Y. A. R., Chauvat, M. P., Ruterana, P., Lahourcade, L., Monroy, E., and Nataf, G., Defect structure in heteroepitaxial semipolar $(11\bar{2}2)$ (Ga,Al)N, *J. Phys.: Condens. Matter.*, vol. **22**, p. 355802, 2010.

de Wit, R., Theory of disclinations: IV. Straight disclinations, *J. Res. Natl. Bur. Stand. – A. Phys. and Chem.*, vol. **77A**, pp. 607–658, 1973.

Dłużewski, P., Maciejewski, G., Jurczak, G., Kret, S., and Laval, J. Y., Nonlinear finite element analysis of residual stresses induced by dislocations in heterostructures, *Comput. Mater. Sci.*, vol. **29**, pp. 379–395, 2004.

Dłużewski, P., Young, T., Dimitakopulos, G., and Komninou, P., Continuum and atomistic modelling of the mixed straight dislocation, *Int. J. Multiscale Comput. Eng.*, vol. **8**, pp. 331–342, 2010.

Erhart, P. and Albe, K., Analytical potential for atomistic simulations of silicon, carbon, and silicon carbide, *Phys. Rev. B*, vol. **71**, p. 035211, 2005.

Galassi, M., Davies, J., Theiler, J., Gough, B., Jungman, G., Alken, P., Booth, M., and Rossi, F., *GNU Scientific Library Reference Manual – Third Edition*, Network Theory Ltd, United Kingdom, 2002.

Hirth, J. P. and Lothe, J., *Theory of Dislocations*, Wiley, New York, 1982.

Kröner, E., *Continuum Theory of Defects*, Physics of Defects, North-Holland, Amsterdam, 1981.

Liu, J. Q., Skowroński, M., Hallin, C., Söderholm, R., and Lendenmann, H., Structure of recombination-induced stacking faults in high-voltage SiC p-n junctions, *Appl. Phys. Lett.*, vol. **80**, pp. 749–751, 2002.

Love, A. E. H., *Mathematical Theory of Elasticity*, Cambridge University Press, Cambridge, 1927.

Maździarz, M., Young, T. D., Dłużewski, P., Wejrzanowski, T., and Kurzydłowski, K. J., Computer modelling of nanoindentation in the limits of a coupled molecular–statics and elastic scheme, *J. Comput. Theor. Nanosci.*, vol. **7**, pp. 1–10, 2010.

Maździarz, M., Young, T. D., and Jurczak, G., A study of the affect of prerelaxation on the nanoindentation process of crystalline copper, *Arch. Mech.*, vol. **63**, no. 5-6, pp. 533–548, 2011.

Persson, P. O. A., Hultman, L., Jacobson, H., Bergman, J. P., Janzén, E., Molina-Aldareguia, J. M., Clegg, W. J., and Tuomi, T., Structural defects in electrically degraded 4h-SiC p+ /n /n+ diodes, *Appl. Phys. Lett.*, vol. **80**, pp. 4852–4854, 2002.

Plimpton, S., Fast parallel algorithms for short-range molecular dynamics, *J. Comput. Phys.*, vol. **117**, no. 1, pp. 1–19, 1995.

Read Jr., W. T., *Dislocations in Crystals*, McGraw-Hill, New York, 1953.

Schoeck, G., The core energy of dislocations, *Acta Metall. Mater.*, vol. **43**, pp. 3679–3684, 1995.

Steeds, J. W., *Introduction to Anisotropic Elasticity Theory of Dislocations*, Clarendon Press, London, 1973.

Stukowski, A., Visualization and analysis of atomistic simulation data with ovito – the open visualization tool (http://ovito.org/), *Modelling Simul. Mater. Sci. Eng.*, vol. **18**, p. 015012, 2010.

Tadmor, E. B. and Miller, R. E., *Modeling Materials: Continuum, Atomistic and Multiscale Techniques*, Cambridge University Press, Cambridge, 2011.

Teodosiu, C., *A Dynamic Theory of Dislocations and its Applications to the Theory of the Elastic Plastic Continuum, in A. Simmonds (Ed.), Fundamental Asects of Dislocation Theory*, Nat. Bur. Stand. Spec. Publ., Washinton D.C., 1970.

Wright, A. F. and Grossner, U., The effect of doping and growth stoichiometry on the core structure of a threading edge dislocation in gan, *Appl. Phys. Lett.*, vol. **73**, pp. 2751–2754, 1998.